9th Int. Conf. on Environmental Degradation of Materials in Nuclear Power Systems - Water Reactors ANS, NACE, TMS, 1.-5. September 1999, Newport Beach, Kalifornien, USA

# European Round Robin on Constant Load EAC Tests of Low Alloy Steel under BWR Conditions



D. Blind, F. Hüttner, A. Wünsche (MPA Stuttgart, Germany)
K. Küster (HEW, Germany)
H.-P. Seifert , J. Heldt (PSI, Switzerland)
A. Roth (Siemens KWU, Germany)
P. Karjalainen-Roikonen, U. Ehrnstén (VTT Manufacturing Technology, Finland)

Abstract

A large range of data exists internationally regarding environmentally-assisted cracking (EAC) of low alloy steel under BWR conditions. This causes a divergence in opinions about the cracking behaviour and, thus, uncertainty in lifetime prediction.
A Round Robin programme on EAC under constant load for a low alloy fine-grained structural steel 20 MnMoNi 5 5 (sim. A 508 Cl. 3, 0.009% S) under simulated BWR conditions was initiated. The main objectives were to find out to what extent different laboratories are able to obtain similar results using nominally identical test parameters, to achieve a better understanding about the range of existing data and to provide reliable data for the safety assessment of operating plants. 4 European laboratories performed 1000 h constant load tests at 289 °C in high purity water containing 0.4 ppm oxygen at stress intensity factors ranging from 25 to 73 MPa$\sqrt{m}$, using 25 mm C(T)-specimens.

Crack growth could not be detected by on-line methods during the tests. However, the fractographic post-test investigations revealed localised EAC areas along the crack front at elongated MnS-inclusions with a growth typically less than 100 µm. Additionally, much smaller localised areas were observed, the appearance of which resembled that of transgranular environmentally-assisted cracking. Based on the local maximum crack extensions, the apparent maximum crack growth rate is $\leq 5.6 \cdot 10^{-8}$ mm/s in the stress intensity factor range between 25 and 73 MPa$\sqrt{m}$.

## Introduction

The assessment of environmentally-assisted cracking (EAC) related to components of the pressure boundary of water cooled nuclear power plants, e. g. the reactor pressure vessel (RPV), is one of the basic tasks for reactor safety. Thus, EAC crack growth under in-service conditions is an important subject of research. It results in a better understanding of EAC and of data to be used in safety evaluations, lifetime predictions as well as in-service inspections.

EAC of low alloy steels includes corrosion fatigue (CF) or strain-induced corrosion cracking (SICC) under cyclic or transient load, e. g. due to start-up, shut-down or operational transients, and stress-corrosion cracking (SCC) under constant load, e. g. during normal steady-state operation. From the predictive point of view regarding reactor safety, cyclic loading is covered by codes, e. g. ASME PVC Section III and XI, whereas the relevance of stress-corrosion cracking is currently still a subject of international discussions.

The published literature on EAC crack growth rates during constant ("active") load control or constant deflection ("passive load") for low alloy steels in oxygenated high temperature water reveals a broad range of data covering approximately 5 orders of magnitude /1-4/. This weakens the applicability of the constant load EAC data for RPVs and is not in line with general in-service experience for boiling water reactor (BWR) RPVs. The observed large range in the crack growth rate is probably due to variations in test type, test performance, equipment and type of specimens as well as due to intrinsic scatter of the crack growth data.

Consequently, a Round Robin programme on EAC under constant load for a low alloy fine-grained structural steel 20 MnMoNi 5 5 (sim. A 508 Cl. 3. 0.009% S) under simulated BWR conditions was initiated. The main objectives were to find out to what extent different laboratories are able to obtain similar results using nominally identical test parameters, achieve a better understanding about the range of existing data and provide reliable data for the safety assessment of operating plants. Four European laboratories participated in the Round Robin project, namely

- MPA Stuttgart, Germany,
- Paul Scherrer Institut (PSI), Switzerland,
- Siemens KWU, Germany and
- VTT Manufacturing Technology, Finland.

This paper presents the results of the Round Robin constant load tests. The participating laboratories are numbered in an arbitrary manner as laboratory 1...4, which does not refer to the order given above.

## Experimental

### Material

The test material was a low alloy, fine-grained structural steel 20 MnMoNi 5 5 (sim. A 508 Cl. 3, 0.009% S), which is used for pressure boundary components, e.g. reactor pressure vessel in nuclear power plants. The actual chemical composition as well as the nominal composition according to the requirements given in the German Code KTA 3201.1 /5/ are presented in Table I. The mechanical properties according to KTA 3201.1 at 20 °C and 300 °C and the actual values at 23 °C and 288 °C are shown in Table II. The heat treatment of the test material was austenisation at 910-920 °C for 4.75 h followed by water quenching and tempering at 640-650 °C for 9 h followed by air cooling.

### Specimens

Fatigue pre-cracked 25 mm C(T) specimens without side grooves were used in the constant load tests. The specimens were manufactured and pre-cracked by Laboratory 1 according to the requirements presented in ASTM E399-90. The orientation of the specimens was T-L.

The pre-cracking of the specimens was performed in air at room temperature to initial $a_0/W$ ratio of 0.5...0.6 using a frequency of 40 Hz and a load ratio (R-value) of 0.1...0.15. The maximum stress intensity factor, $K_I$, at the end of pre-cracking was lower than 22 MPa$\sqrt{m}$. After pre-cracking, the specimens were cleaned in an ultrasonic bath with ethanol for approx. 10 min, dried in air and sent to the other participating laboratories for constant load testing.

### Test Parameters

The 1000 h constant load tests were performed under simulated BWR conditions in accordance to the test parameters presented in Table III. In all, 12 specimens loaded to nominal initial $K_I$ values of 25, 35, 45, 55, 65 and 70 MPa$\sqrt{m}$ were tested.

The nominal test environment was pressurised (9 MPa) high-temperature, high-purity water at 289 °C with a nominal, adjusted, inlet dissolved oxygen content of 0.4 ppm. The target water conductivity was < 0.08 µS/cm and < 0.2 µS/cm, respectively, in the inlet and outlet water at ambient temperature.

### Experimental Set-up

Two specimens were tested simultaneously in a daisy chain assembly in an autoclave connected to a recirculation loop in Laboratories 1, 3 and 4 or to once through system in Laboratory 2 with a water exchange rate of 0.5...2 /h in every other laboratory except in Laboratory 1 once every 15 h. The specimens were electrically isolated from each other as well as from the autoclave body by $ZrO_2$ or MgO stabilised $ZrO_2$.

Autoclaves with integrated tensile testing machines (screw driven or servo-hydraulic) for loading were used. All experimental parameters were continuously monitored using data acquisition systems. Beside the test parameters like inlet/outlet oxygen content, inlet/outlet conductivity, pressure, load, autoclave temperature, the following values were registered:

- The electrochemical corrosion potential (ECP) was measured in all laboratories using an external, water cooled Ag/AgCl/$H_2O$ reference electrode, which has no chloride containing filling solution and relies on the natural solubility of AgCl. Additionally an external, pressure balanced Ag/AgCl/0.01 M KCl reference electrode was used in Laboratory 4.
- The redox potential was measured using a Pt-electrode in Laboratories 2, 3 and 4.
- The pH at ambient temperature was monitored in

Laboratories 2 and 4.

- The crack growth was monitored using the reversed direct current potential drop (DC-PD) technique in Laboratories 2 and 4.
- The crack mouth opening displacement (CMOD) was monitored in Laboratory 1. The stroke of the pull rod was registered in Laboratories 3 and 4.

Test Procedure

The constant load tests were performed at all participating laboratories under nominally identical conditions as defined in the test specification. After assembling 2 pre-cracked specimens in a daisy chain, the autoclave was filled with pure water, bubbled with nitrogen or argon in order to remove excessive oxygen and heated up to 289 °C with a heating rate of 10 °C/h. When the temperature was achieved the oxygen content of the inlet water was adjusted to 0.4 ppm. In Laboratory 1 the adjustment to the oxygen content of 0.4 ppm was done before heating. To achieve stable conditions with respect to water chemistry, electrochemistry and oxide film formation, the specimens were preconditioned using a pre-load of 9 kN (0 kN at Laboratory 4) for at least one week prior to the constant load test. After the preconditioning, the load was increased with a ramp of 20 kN/h to the load related to the target $K_I$-value and then held at a constant level. In Laboratory 1 the load was applied stepwise with approx. 5 kN/10 min. All tests were performed under load control.

During the conditioning and the constant load phases, water grab samples were taken from the inlet and outlet water at least once a week. The water grab samples were analysed both by the individual laboratories and by Laboratory 1 for e.g. ions $Cl^-$, $SO_4^{2-}$, $PO_4^{3-}$ using ion-chromatography. Also the total organic carbon (TOC) was determined.

After 1000 h at constant load, the specimens were unloaded to 9 kN or 0 kN (Laboratory 4), the heating was stopped and the pressure was decreased. The specimens were disassembled, cleaned with ethanol, dried and sent to Laboratory 1.

The cracks in the specimens were opened after cooling in liquid nitrogen. Six of the twelve specimens (tested in Laboratories 1 and 4), were dry cut into two pieces along a plane perpendicular to the crack plane and parallel to the side faces. One half was kept for metallographical investigations. The crack in the other half was opened after cooling in liquid nitrogen. Before starting the investigation of the fracture surfaces with SEM, the oxide layer was removed by galvanostatic reduction in an ENDOX-bath /6/. Each laboratory investigated the fracture surface of one half of the specimens they had tested. Laboratory 1 investigated the other halves of all tested specimens.

Post-test determination of crack growth

The crack growth was determined from each specimen in connection to detailed fractographic investigations using a scanning electron microscope, SEM. The whole crack front was investigated in steps of approximately 0.25 mm, and the maximum crack extension at each field of observation was measured and documented at magnifications of 500 and 1000, or higher. Laboratories 2, 3 and 4 measured the maximum crack extension perpendicular to the prefatigue crack front while Laboratory 1 measured the crack extension along the microscopic crack growth direction. In addition to crack growth, also MnS-inclusions and anomalies were reported. For each specimen the maximum and average crack extensions were calculated. The maximum crack extension is the deepest observed local crack extension along the investigated crack front. The average crack extension is the arithmetic mean value of all measurements along the investigated crack front including measurement points without detectable crack extension.

## Results

Experimental parameters

An overview of the average values of environmental and other experimental parameters of all tests is presented in Table IV. The temperature varied between 286...291 °C and the pressure varied between 9...10.3 MPa during the tests in the participating laboratories. The inlet oxygen content of 0.38...0.41 ppm resulted in an outlet oxygen content between 0.29 and 0.38 ppm in the different laboratories caused by different oxygen consumption in the loop systems. The inlet conductivity was between 0.06 and 0.08 µS/cm, while the outlet conductivity of the water (at 25 °C) was between 0.11 and 0.27 µS/cm. The average outlet content of $Cl^-$-ions was between 1.3 and 3.2 ppb in Laboratories 1, 3 and 4 and 12.5 ppb in Laboratory 2. The $SO_4^{2-}$ -content was typically below 1 ppb in all laboratories.

*Redox potential* The averaged redox potential values in Laboratories 2, 3 and 4 were between + 20 mV and + 70 mV measured against the $Ag/AgCl/H_2O$ reference electrode. The redox potentials are similar in Laboratories 2 and 4, while Laboratory 3 measured slightly higher redox potentials. The redox potential measured against an external, pressure balanced Ag/AgCl/0.01 M KCl-electrode was +205 $mV_{SHE}$ on the standard hydrogen scale in Laboratory 4.

*Corrosion Potentials* The averaged electrochemical corrosion potentials measured against the external water cooled $Ag/AgCl/H_2O$ reference electrode varied between -118 mV and -280 mV. The measured potential in Laboratories 3 and 4 were similar (between -118 mV and -127 mV) being higher than the lower value measured in Laboratory 2 (between -173 and -121 mV) and the values measured in Laboratory 1 (between -200 and -280 mV). The corrosion potential measured by Laboratory 4 using an external, pressure balanced Ag/AgCl/0.01 M KCl electrode was + 69 $mV_{SHE}$ when the average outlet oxygen concentration was 0.33 ppm. The variation of the measured corrosion potential was typically less than 50 mV during each test.

Fractography and crack growth

In the fractographic investigations, local EAC areas were observed at elongated manganese sulphide (MnS) inclusions at a few sites in most specimens (typically less than 4 sites/specimen), see Figure 1. The crack extension at these locations was typically below 100 µm.

In addition to these general observations concerning all specimens, some specific observations were made in the fractographic investigations. These are described in the following. In addition to the transgranular EAC areas around the elongated

MnS inclusions local, very small transgranular areas were observed at several locations along the crack front in 6 specimens (tested in Laboratories 1 and 4). The extension at these locations was typically less than 30 µm, and the size was too small for definite verification of the cracking mechanism. However, their appearance resembles that of environmentally-assisted cracking, see Figure 2. Manganese sulphides, or traces of former MnS were occasionally, but not always, seen in the vicinity of these areas. The extensions of these areas are included in the values reported in Table V.

A smooth zone, about 10 µm wide, was observed directly after the pre-cracked area in the specimens tested in Laboratory 2, see Figure 3. The size of this zone was slightly larger in the specimen tested at the higher stress intensity level. This zone did not exhibit features typical for EAC, and was therefore not included in the crack extension measurements.

Some branching was found near the tip of the pre-crack in two specimens with the constant load $K_I$-value of 32 and 55 MPa$\sqrt{m}$ tested in Laboratories 1 and 4, respectively. A cross-section of the C(T) specimen tested using $K_I$ = 55 MPa$\sqrt{m}$ with such branching revealed several short secondary cracks along the pre-crack and a branched crack tip. The length of the branches was about 50 µm and they were filled with oxide.

No crack growth was observed by any of the participating laboratories based on the continuous monitoring of crack growth during the constant load testing, using either DC-PD measurement or CMOD measurement.

A summary of the reported crack extensions (maximum and average), measured using SEM by the participating laboratories as well as the parallel measurements by Laboratory 1 is presented in Table V. The corresponding apparent crack growth rates are presented in Table VI. Because neither origin nor time of EAC could be conclusively confirmed, all reported crack growth rates are considered to be apparent crack growth rates.

The maximum crack extension was found to increase with the stress intensity from below or equal to 20 µm at the lowest stress intensity ($K_I$ = 25 MPa$\sqrt{m}$) and resulting in a single peak value of 200 µm at the stress intensity $K_I$ = 55 MPa$\sqrt{m}$, Table V. The maximum crack growth rates were below $5.6 \cdot 10^{-8}$ mm/s in the stress intensity range between 25...73 MPa$\sqrt{m}$, Table VI. The average crack extension was less than 1 µm at 25 MPa$\sqrt{m}$ and raised to 13 µm at 73 MPa$\sqrt{m}$, Table V. Crack extensions and crack growth rates as a function of stress intensity factor are presented in Figures 4...7.

## Discussion

Twelve constant load tests on fine-grained low alloy steel were performed in four different European laboratories in a nominally similar, simulated BWR-environment using 25 mm C(T) specimens and stress intensities between 25 MPa$\sqrt{m}$ and 70 MPa$\sqrt{m}$. No crack growth was observed based on the on-line crack length measurements during the tests. However, the fractographic post-test investigations revealed few, local EAC areas at MnS inclusions as well as small, localised areas along the crack front, the appearance of which resembled that of transgranular environmentally-assisted cracking. It should be noted that only half of the full width was fractographically investigated in 6 specimens. Thus, it is possible that the actual maximum crack extension went undetected. Due to the local nature of these areas it is understandable that crack growth during the constant load test could not be detected by the on-line technique. Thus, it cannot be stated, when these local areas have developed. The areas may indicate a transient behaviour and it is possible that they will not result in stable crack growth. Due to the limited testing time of about 1000 h and the uncertainty of time or origin of EAC, crack growth cannot be totally excluded. Results from other studies using similar tests /4, 9/ suggest that cracking due to EAC may be limited to the very early stage in crack growth experiments, probably even to the rising load period at the beginning of the constant load test. This could be further investigated by initiating crack growth in the autoclave by fatigue loading using low frequency and high R-values before applying constant load. The lack of evidence of stable, continuous crack growth in the 1000 h tests indicates that the test material does not show pronounced susceptibility to EAC under BWR conditions.

During exposure to high temperature oxidising water, all surfaces will oxidise, including both the fracture surface of the pre-crack and of an eventual growing crack. This results in a loss of micro-fractographic details and causes uncertainty in interpretation of small localised fractographic areas. Crack advance large enough to be measured by on-line monitoring and/or larger than the characteristic features of the material in question (e.g. grain size) would result in higher reliability of crack growth determination. The large difference in the reported maximum crack extensions between the testing laboratory and Laboratory 1 is due to the fact that the crack extension is measured along the macroscopic or microscopic crack growth direction by Laboratories 2, 3 or 4 and by Laboratory 1, respectively. This causes corresponding differences in apparent crack growth rates partly explaining the typical scatter of about 1 order of magnitude in da/dt vs. $K_I$ results. The maximum crack growth rates obtained here are conservatively calculated from the observed localised maximum crack extensions.

EAC was only observed at elongated MnS inclusions at few locations along the crack front. Manganese sulphide inclusions were occasionally observed in the vicinity of the possible localised, small EAC areas. MnS is known to dissolve in BWR environment resulting in acidification of the crack tip environment and consequent enhancement of the crack growth /8/.

The apparent maximum crack growth rate calculated based on these localised transgranular areas, i.e. $5.6 \cdot 10^{-8}$ mm/s lies in the lower range of the literature crack growth rate data /1, 4, 9/. The observed maximum crack growth rate is more than three orders of magnitude below the maximum rate of approx. $1 \cdot 10^{-4}$ mm/s which may be derived from published data /1/.

The performed crack growth experiments under specified and well controlled conditions resulted in reproducible results. This indicates, that the observed range in published crack growth data is mainly not due to scatter but rather due to different experimental conditions.
All participating laboratories achieved most of the defined testing conditions and were able to sustain stable testing conditions during the constant load tests. The effect of minor differences

during heating and preconditioning in the different laboratories on crack initiation and growth could not be evaluated due to the lack of stable crack growth. In addition to differences in interpretation of the fracture surfaces, the main differences between the laboratories were in the measured outlet conductivity and the corrosion potential. The main contribution to the outlet conductivity is most probably due to release of chromate from the materials in the autoclave, although an average $Cl^-$ content of above 10 ppb also will notably increase the outlet conductivity. Higher corrosion potentials measured against the external, water cooled $Ag/AgCl/H_2O$ reference electrode under nominally similar conditions were obtained in laboratories with higher water exchange rate. The flow rate of the water is known to affect the measured corrosion potential values. Especially with low flow rates the local oxygen content near the specimen may be different from the bulk water oxygen content resulting in lower corrosion potentials than expected based on the outlet oxygen concentration. The corrosion potential measured against an external, pressure balanced Ag/AgCl/0.01 M KCl reference electrode was about +70 $mV_{SHE}$, which is in good agreement with values reported in the literature /7/. Both reference electrodes used by the laboratories behaved in a stable manner during the test, with a change typically less than 50 mV. This change includes both an eventual small drift due to the electrodes as well as small changes in the environmental conditions during the test (e.g. a small increase of oxygen concentration in the outlet water).

## Conclusions

Based on the results of the Round Robin constant load tests for the low alloy, fine-grained steel 20 MnMoNi 5 5 (sim. A 508 Cl.3, 0.009% S) in simulated a BWR environment with 0.4 ppm $O_2$ in the inlet water at stress intensity factor levels between 25 and 73 MPa$\sqrt{m}$, the following conclusions can be drawn:

- Crack growth experiments under specified and well controlled conditions resulted in reproducible results. This indicates, that the observed range in published crack growth data is not due to scatter but rather due to different experimental conditions.
- No evidence of stable, continuous environmentally-assisted crack growth were found in the 1000 h constant load tests.
- Local EAC was only observed at elongated MnS inclusions at few locations along the crack fronts of the specimens
- Additional small areas with possible EAC were localised along the crack front. Manganese sulphide inclusions were occasionally observed near these areas. The size of these areas was too small for a definite determination of the cracking mechanism.
- Based on a conservative interpretation of the results, initiation of transgranular environmentally-assisted cracking can not be excluded during 1000 h constant load tests under the above conditions.
- The calculated apparent crack growth rate, based on the maximum extension of the local transgranular areas were very low, lying below $5.6 \cdot 10^{-8}$ mm/s for $K_I$ lower than 73 MPa$\sqrt{m}$.
- Higher corrosion potentials measured against the external, water cooled $Ag/AgCl/H_2O$ reference electrode under nominally similar conditions were obtained in laboratories with higher water exchange rate.


## Acknowledgements

MPA Stuttgart as well as other partners express gratitude to the Technische Vereinigung der Großkraftwerksbetreiber e.V. (VGB) for its support of the Round Robin.
PSI thanks the Swiss Federal Nuclear Safety Inspectorate (HSK) and the Swiss Federal Office of Energy (BFE) for the promotion of this project.
Swedish Nuclear Inspectorate, SKI, is gratefully acknowledged for its financial support which enabled VTT Manufacturing Technology to take part in the Round Robin.


## References


1. F. P. Ford, P. L. Andresen, Stress Corrosion Cracking of Low Alloy Steels in 288 °C Water. Corrosion '89, New Orleans, Luisiana, April 17-21, (1989), Paper 498. 19.
2. M. O. Speidel, R.M. Pedrazzoli, Ursachen und Geschwindigkeit des umgebungsabhängigen Bruch in metallischen und nichtmetallischen Werkstoffen, In: M. Schaper, J. Barthel: Umgebungsabhängiges Bruchverhalten, DGM-Informationsgesellschaft, Oberursel, (1991).
3. D. Blind et al., Korrosionsuntersuchungen an niedriglegierten Feinkornbaustählen für Kraftwerksanlagen, Abschlußbericht des BMBF Forschungsvorhabens 1500 826, Staatliche Materialprüfanstalt Stuttgart, 12/1995.
4. K. Kußmaul, D. Blind D., V. Läpple, New observations on the crack growth rate of low alloy nuclear grade ferritic steels under constant active load in oxygenated high-temperature water, Nuclear Engineering and Design, 168, (1997), 53-75.
5. KTA 3201.1, Komponenten des Primärkreislaufes von Leichtwasserreaktoren: Teil Werkstoff, Anhang A, Tabelle A1-1
6. B. Goubau, H. Werner, Untersuchungen zur mikrofraktografischen Beurteilung von magnetitbelegten Bruchflächen, Praktische Metallografie 17 (1980), 209-219.
7. EPRI Report NP-2853, The general and localized corrosion of carbon and low-alloy steels in oxygenated high-temperature water, February (1983)
8. H. Hänninen, W. Cullen, M. Kemppainen, Effects of MnS inclusion dissolution on environmentally assisted cracking in low alloy and carbon steels. Corrosion '89, New Orleans, Luisiana, April 17-21, (1989), Paper 565. 19.
9. J. Heldt, H.-P. Seifert, Stress Corrosion Cracking of Reactor Pressure Vessel Steels under Boiling Water Reactor Conditions. This conference.


Table I: Chemical composition of the test material 20 MnMoNi 5 5 (sim. A 508 Cl. 3, 0.009% S),

| Element [wt%] | C | Si | Mn | P | S | Cr | Mo | Ni | Al | Cu | V | Sn | N | As |
|---|---|---|---|---|---|---|---|---|---|---|---|---|---|---|
| KTA 3201.1 | 0.15-0.25 | 0.10-0.35 | 1.15-1.55 | max 0.012 | max 0.012 | max 0.20 | 0.40-0.55 | 0.45-0.85 | 0.01-0.04 | max 0.12 | max 0.02 | max 0.011 | max 0.013 | max 0.0025 |
| Actual * | 0.20 | 0.16 | 1.24 | 0.008 | 0.009 | 0.09 | 0.50 | 0.78 | 0.01 | 0.06 | 0.01 | < 0.01 | n.d.** | n.d.** |

* determined by Laboratory 1 ** not determined

Table II: Mechanical properties of the test material 20 MnMoNi 5 5 (sim. A 508 Cl. 3, 0.009% S)

| Temperature [°C] | Yield Strength [MPa] | Ultimate Tensile Strength [MPa] | Young's Modulus [MPa] | Elongation to Fracture [%] | Reduction of Area [%] |
|---|---|---|---|---|---|
| 20* | ≥ 390 | ≥ 505 | 211000 | ≥ 18 | - |
| 300* | ≥ 353 | ≥ 505 | 192000 | ≥ 16 | - |
| 23** | 465 | 594 | 213000 | 23 | 61 |
| 288** | 430 | 631 | 204600 | 22 | 51 |

* according to KTA 3201.1
** determined by Laboratory 1

Table III: Nominal test parameters for the 1000 hours constant load tests.

| | Lab 1 | Lab 2 | Lab 3 | Lab 4 |
|---|---|---|---|---|
| Material | 20 MnMoNi 5 5 (sim. A 508 Cl.3, 0.009 %S) | | | |
| Specimens | 25 mm C(T) without side grooves | | | |
| Environment | Pure water, quasi-stagnant, T = 289 °C<br>$O_2$ = 0.4 ppm (inlet), κ < 0.08 µS/cm (inlet), κ < 0.2 µS/cm (outlet) | | | |
| Stress intensity factor [MPa√m] | 25<br>35<br>65<br>70 | <br><br>45<br>55 | 25<br>35<br>45<br>55 | <br><br>45<br>55 |

Table IV: Summary of nominal and average testing parameters measured during the constant load tests.

| Parameter | | | Nominal values | Lab. 1 test 1 | Lab. 1 test 2 | Lab. 2 test 1 | Lab. 3 test 1 | Lab. 3 test 2 | Lab. 4 test 1 |
|---|---|---|---|---|---|---|---|---|---|
| Oxygen inlet | [ppm] | | 0.4 | 0.38 | 0.4 | 0.41 | 0.40 | 0.40 | 0.40 |
| Oxygen, outlet | [ppm] | | 0.4 | 0.3 | 0.35 | 0.38 | 0.32 | 0.29 | 0.33 |
| Conductivity, inlet | [µS/cm] | | < 0.08 | 0.057 | 0.062 | 0.056 | 0.06 | 0.06 | 0.08 |
| Conductivity, outlet | [µS/cm] | | < 0.2 | <0.2 | 0.2 | 0.27 | 0.15 | 0.20 | 0.11 |
| $Cl^-$ -content, inlet<br>$Cl^-$ -content, outlet | [ppb] | | | 0.7<br>0.8 | 1<br>1 | 2.4<br>12.5 | 1.3<br>1.3 | 1.3<br>1.7 | 1.8<br>2.5 |
| Temperature | [°C ] | | 289 | 291 | 290 | 286 | 289 | 288 | 288 |
| Pressure | [MPa] | | 9 | 9.45 | 9.3 | 10.3 | 9.0 | 9.1 | 9.1 |
| Water exchange rate | [$h^{-1}$] | | | 0.07 | 0.07 | 0.5 | 1.5 | 1.4 | 2 |
| Flow rate | [l/h] | | | 14 | 14 | 0.5 | 15 | 14 | 24 |
| Corrosion potential vs Ag/AgCl/$H_2O$ * | [mV] | spec. 1<br>spec. 2 | - | -260<br>-280 | -200<br>-220 | -173<br>-121 | -127<br>-125 | -123<br>–125 | -118 |
| Corrosion potential vs Ag/AgCl/0.01 M KCl** | [$mV_{SHE}$ ] | | - | | | | | | +69*** |
| Redox potential vs Ag/AgCl/$H_2O$ * | [mV] | | | | | + 20 | + 70 | + 45 | + 21 |
| Redox potential vs Ag/AgCl/0.01 M KCl** | [$mV_{SHE}$] | | | | | | | | +205*** |
| pH at ambient temperature | | | | | | 6.2 (outlet) | | | 6.9 (inlet) |
| Stress intensity factor | [MPa√m] | spec. 1<br>spec. 2 | | 25<br>32 | 68<br>73 | 45<br>56 | 25<br>34 | 44<br>55 | 45<br>56 |

* External, water cooled Ag/AgCl/$H_2O$ reference electrode
** External, pressure balanced Ag/AgCl/0.01 M KCl reference electrode
*** calculated as $U_{SHE} = U_{meas} + A$, where $A = 0.3434185 - 1.00569\ 10^{-3}\ (T-25\ °C) + 5.4081\ 10^{-7}\ (T-25°C)^2 - 5.49061\ 10^{-9}\ (T-25°C)^3 - 0.007$

Table V: Maximum and average crack extensions measured on the fracture surfaces after the constant load tests

| Laboratory | Stress intensity factor $K_I$ [MPa√m] | Constant load test duration [h] | Maximum crack extension $\Delta a_{max}$ [µm] | | Average crack extension $\Delta a_{ave}$ [µm] | |
|---|---|---|---|---|---|---|
| | | | Testing lab* | Lab 1 | Testing lab* | Lab 1 |
| Lab. 1 | 25 | 1009 | 20 | | 1 | |
| | 32 | 1009 | 30 | | 1 | |
| | 68 | 998 | 80 | | 6 | |
| | 73 | 998 | 50 | | 13 | |
| Lab. 2 | 45 | 1060 | 60 | 15 | -** | 1 |
| | 56 | 1060 | 100 | 20 | -** | < 0.5 |
| Lab. 3 | 25 | 1008 | *** | 10 | *** | < 0.5 |
| | 34 | 1008 | *** | 10 | *** | < 0.5 |
| | 44 | 988 | *** | 50 | *** | 2 |
| | 55 | 988 | 200 | 65 | 4 | 4 |
| Lab. 4 | 45 | 1006 | 41 | 50 | 11 | 7 |
| | 56 | 1006 | 46 | 70 | 6 | 8 |

* laboratory at which the test was performed
** no calculation of average values
*** local areas ≤ 30 µm without any characteristic fractographic features and clear indications for EAC. The ongoing oxidation during test results in a significant loss of micro-fractographic details. The resulting EAC resolution limit is therefore estimated to be ca. 30 µm by Laboratory 3.

Table VI: Maximum and average crack growth rates after the1000 h constant load test

| Laboratory | Stress intensity factor $K_I$ [MPa√m] | Maximum crack growth rate $(\Delta a/\Delta t)_{max}$ [mm/s] | | Average crack growth rate $(\Delta a/\Delta t)_{ave}$ [mm/s] | |
|---|---|---|---|---|---|
| | | Testing lab * | Lab 1 | Testing lab * | Lab 1 |
| Lab. 1 | 25 | $5.5 \cdot 10^{-9}$ | | $2.8 \cdot 10^{-10}$ | |
| | 32 | $8.3 \cdot 10^{-9}$ | | $2.8 \cdot 10^{-10}$ | |
| | 68 | $2.2 \cdot 10^{-8}$ | | $1.7 \cdot 10^{-9}$ | |
| | 73 | $1.4 \cdot 10^{-8}$ | | $3.6 \cdot 10^{-10}$ | |
| Lab. 2 | 45 | $1.6 \cdot 10^{-8}$ | $3.9 \cdot 10^{-9}$ | ** | $2.6 \cdot 10^{-10}$ |
| | 56 | $2.6 \cdot 10^{-8}$ | $5.2 \cdot 10^{-9}$ | ** | $< 1.5 \cdot 10^{-10}$ |
| Lab. 3 | 25 | no CG | $2.8 \cdot 10^{-9}$ | no CG | $< 1.5 \cdot 10^{-10}$ |
| | 34 | no CG | $2.8 \cdot 10^{-9}$ | no CG | $< 1.5 \cdot 10^{-10}$ |
| | 44 | no CG | $1.4 \cdot 10^{-8}$ | no CG | $5.6 \cdot 10^{-10}$ |
| | 55 | $5.6 \cdot 10^{-8}$ | $1.8 \cdot 10^{-8}$ | $1.1 \cdot 10^{-9}$ | $1.1 \cdot 10^{-9}$ |
| Lab. 4 | 45 | $1.1 \cdot 10^{-8}$ | $1.4 \cdot 10^{-8}$ | $3.0 \cdot 10^{-9}$ | $1.9 \cdot 10^{-9}$ |
| | 56 | $1.2 \cdot 10^{-8}$ | $1.9 \cdot 10^{-8}$ | $1.7 \cdot 10^{-9}$ | $2.2 \cdot 10^{-9}$ |

* laboratory at which the test was performed
** no calculation of average values
*** no CG= below the resolution limit of the EAC ca. 30 µm by Laboratory 3, see Table V.

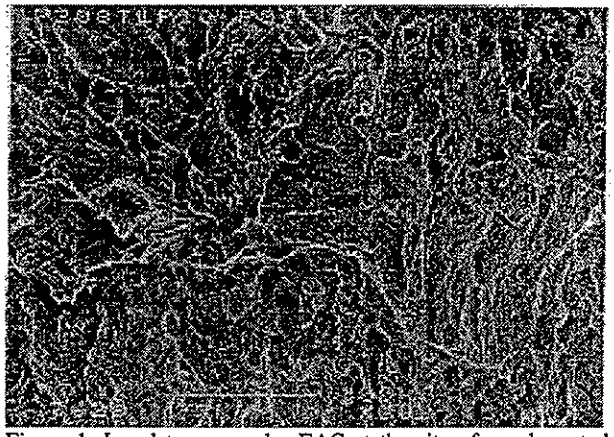

Figure 1: Local transgranular EAC at the site of an elongated MnS inclusion, $K_I = 55$ MPa$\sqrt{m}$.

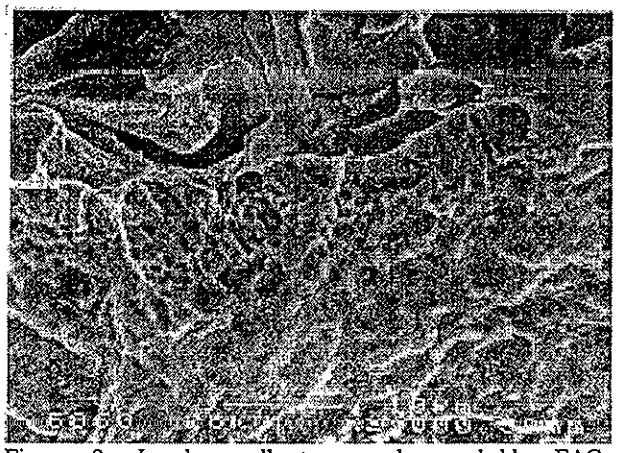

Figure 2: Local, small transgranular probable EAC, $K_I = 56$ MPa$\sqrt{m}$.

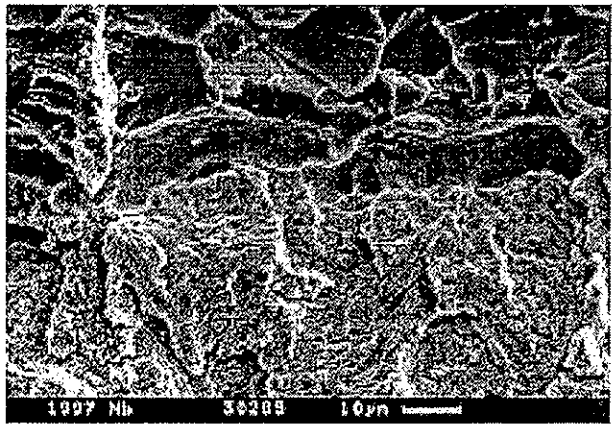


Figure 3 Smooth zone after the precrack tip, $K_I = 56$ MPa$\sqrt{m}$ .

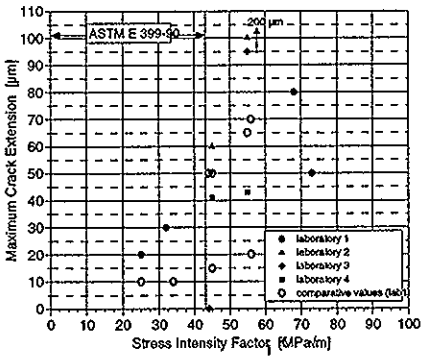


Figure 4: Maximum crack extension vs. stress intensity factor

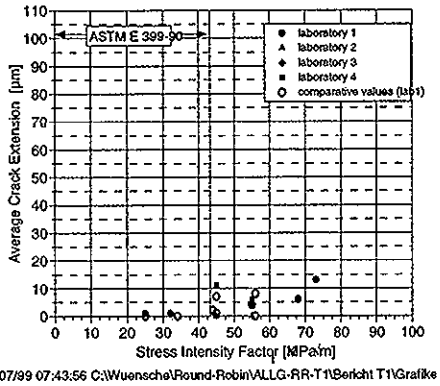


Figure 5: Average crack extension vs. stress intensity factor

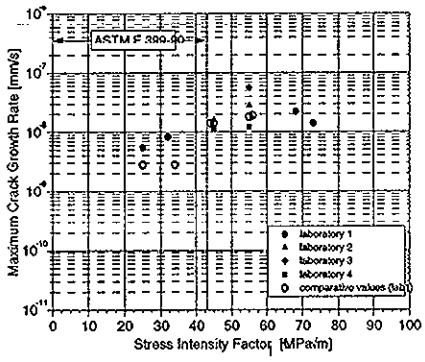


Figure 6: Maximum crack growth rate vs. stress intensity factor

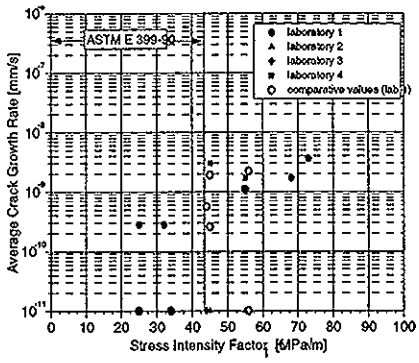


Figure 7: Average crack growth rate vs. stress intensity factor